Mechanics of Advanced Composite Structures 6 (2016) 113-121

Semnan University

Mechanics of Advanced Composite Structures

journal homepage: http://MACS.journals.semnan.ac.ir

Mechanical Properties of CNT-Reinforced Polymer Nanocomposites: A Molecular Dynamics Study

M. Farhadinia [a], B. Arab [b,c*], J.E. Jam [a]

[a] *Composite Materials and Technology Center, Malek Ashtar University of Technology, Tehran, Iran*
[b] *Department of Mechanical Engineering, Faculty of Engineering, Tehran North Branch, Islamic Azad University, Tehran, Iran*
[c] *Young Researchers and Elites Club, Tehran North Branch, Islamic Azad University, Tehran, Iran*

PAPER INFO

Paper history:
Received: 2016-04-24
Revised: 2016-08-05
Accepted: 2016-08-23

Keywords:
Carbon nanotubes
Polymer nanocomposites
Mechanical properties
Molecular dynamics

ABSTRACT

Understanding the mechanism underlying the behavior of polymer-based nanocomposites requires investigation at the molecular level. In the current study, an atomistic simulation based on molecular dynamics was performed to characterize the mechanical properties of polycarbonate (PC) nanocomposites reinforced with single-walled armchair carbon nanotubes (SWCNT). The stiffness matrix and elastic properties such as Young's modulus, shear and bulk moduli, and Poisson's ratio for the pure PC and PC/CNT nanocomposites were estimated using the constant-strain method. In this research, this method was used for the first time to investigate the effects of different parameters, such as the effects of weight fraction and aspect ratio of CNTs on the elastic properties of PC/SWCNT nanocomposites. From the computational results, the elastic moduli of PC/CNT nanocomposites increased with increasing the amount of incorporated CNTs, while their aspect ratio (l/d) also increased. A significant increase in the elastic modulus (41.2%) was observed, even with the addition of a small quantity (2.4 wt%) of SWCNTs. Upon addition of about 6.9 wt% of SWCNTs, the elastic modulus increased by almost 52%.

1. Introduction

Polymer nanocomposites have the potential to provide significant increases in specific strength-to-weight and stiffness-to-weight ratios compared with unreinforced polymers. Polycarbonates (PCs) are an extremely useful class of transparent thermoplastic polymers known for their toughness and clarity, which are widely used in various engineering applications. Because of their optical clarity, light weight, high impact resistance, and good molding ability, PC is predominantly used in transparent armor, protective eye wear, and automobile and air craft transparencies [1]. Future bullet-proof vests and defense gear, in particular, aim towards greater fracture toughness and strength in a material that can absorb and dissipate large amounts of energy before failure [2]. The duel capabilities to resist impact and high temperatures makes PC a suitable candidate for common applications in house wares, laboratories, and industries, and it is also the object of academic research due to its widespread usage and unusual properties.

In the ongoing research in composite science and technology, carbon nanotubes (CNTs) have earned special attention due to their high strength, high ductility, light weight, and exceptional mechanical, thermal, optical, and electrical properties. Combined with their low density and high aspect ratios, CNTs are ideal fillers for fabricating light-weight polymer composite materials with improved mechanical performance and multifunctional properties. By incorporating CNTs into PC, the resulting material's strength and fracture toughness can be significantly improved. The level of reinforcement depends upon several factors, such as the type of CNT, surface modification, CNT orientation, the amount of CNTs, and polymer/nanotube interfacial bonding [2].

In recent years, PC/CNT nanocomposites have been investigated through a number of experimental studies. For example, Liu et al. [3] reported

* Corresponding author, Tel.: +98-21-22970274; Fax: +98-21-22970274

E-mail address: b.arab@iau-tnb.ac.ir

that with 3 wt% of multi-walled carbon nanotubes (MWCNTs) added to PC, the tensile strength of the composite increased by about 40% compared to pure PC. However, adding 5 wt% of MWCNTs to PC caused a significant reduction in the material's strength. Eitan et al. [4] used bisphenol-A-PC with MWCNTs as sample composites for mechanical characterization. Tensile tests were performed, and for composites with surface-modified MWCNTs (5 wt%), the modulus improved by 95% in comparison to pure PC. Even for composites using pristine MWCNTs (5 wt%), the modulus was enhanced by nearly 70% in comparison to pure PC. Chen et al. [5] carried out a study on the mechanical properties of PC composites containing 1–8 wt% of MWCNTs. With increasing the MWCNT content, significant improvements in the elastic moduli were observed.

The extent to which mechanical reinforcement can be achieved depends on several factors, which are difficult to control within experimental studies. For this reason, theoretical studies based on analytical and computational methods have been widely applied to the study of polymer/CNT nanocomposites. The main goal of computational materials' science is the rapid and accurate prediction of properties of new materials prior to their development and production. New methods have emerged as an alternative to the traditional experimental and theoretical methods for estimating mechanical properties of nanomaterials. In this regard, several theoretical studies have recently been performed specifically on polymer/CNT nanocomposites, investigating different aspects of these interesting materials. For example, Aghadavoudi et al. [6] used a molecular dynamics (MD) method to investigate the effects of resin cross-linking ratios on the mechanical properties of CNT-reinforced epoxy-based nanocomposites. The cross-linking ratio was found to have no significant effect on resin density, while the nanocomposite's Young's moduli, especially in the transverse direction, increased with increases in the resin's cross-linking ratio. In addition, the CNT diameter was observed to have a strong influence on nanocomposite longitudinal and transverse moduli. Arash et al. [7] studied the mechanical behavior of CNT/PMMA composite materials subjected to tensile loading using MD simulations. The effect of the aspect ratio of CNTs on the elastic properties of the nanocomposites and the interfacial region between nanotubes and the polymer matrix was investigated. It was revealed that a PMMA-based composite reinforced with an infinitely long (5, 5) CNT was significantly stiffer than a pure PMMA polymer. Furthermore, the CNT/polymer interfacial strength increased by increasing the aspect ratios of CNTs, leading to higher stiffness values.

Sharma et al. [8] studied the mechanical and thermal properties of MWCNT/PC nanocomposites, through MD simulations. Up to an 89% increase in the elastic modulus was observed, even with the addition of a small quantity (up to 2 wt%) of MWCNTs. Upon addition of about 2% volume of MWCNTs, the elastic modulus increased by almost 10%. Gates et al. [9] provided an approach for multiscale modeling and simulation of advanced materials, such as nanotube-reinforced polymer composites for structural applications. Odegard et al. [10] evaluated the effective elastic properties of CNT-reinforced nanocomposites using MD-based multiscale approaches. They combined the MD method with micromechanics, based on their previously developed equivalent-continuum model [11]. In another study, Rossi and Meo [12] proposed a finite element (FE) model of single-walled carbon nanotubes (SWNTs), based on molecular mechanics, and they investigated mechanical properties, such as the Young's modulus and the materials' ultimate strength. In addition, Papanikos et al. [13] utilized an atomistic-based FE model to evaluate the geometrical characteristics and elastic properties of the beams with the same tensile, bending, and torsional behavior as the CNTs. They assumed a linear behavior for the load–displacement relationship of the C–C bonds, which made the presented results acceptable for small strains in SWCNT. Tserpes et al. [14] proposed a multiscale representative volume element (RVE) of SWCNT-reinforced nanocomposites, with perfect bonding between the nanotube and the matrix, until the interfacial shear stress exceeded the bonds' corresponding strength.

Study of the properties and behavior of polymer nanocomposites involves several length and time scales, for example, the behavior of such materials at the upper scales is dramatically influenced by the phenomena occurring at the lower scales. Therefore, the ability of predictive modeling and simulation of various scales would be of great importance for development of polymer nanocomposites. Well-validated computational methods, such as molecular dynamics, can be effectively employed to gain knowledge about the basic phenomena occurring at the atomic scale. This method has been used to study various polymer systems reinforced with nano-fillers. To the authors' knowledge, however, there is no comprehensive atomistic simulation study on CNT-reinforced PCs, as an important engineering material. The current study used classical molecular dynamics to estimate the mechanical properties of PC/CNT nanocomposites, considering different weight fractions and nanotube aspect ratios.

2. Methods

2.1. Simulation Procedure

Molecular dynamics, as a powerful and modern tool for numerical study of materials, is based on solving the classical Newton's equation of motion. It involves the determination of the time evolution of a set of interacting atoms, followed by integration of the corresponding equations of motion [15]. The molecular configurations, stored at different time steps of simulation, form the possible phase state configurations of the molecular system, following the principles of statistical mechanics. Molecular dynamics' simulations are usually performed based on classical interatomic potential, which can often be derived from quantum mechanics' calculations [16]. The accuracy of MD simulations is intrinsically dependent on the quality of the empirical potential energy functions and the force-field parameters used [17]. A force-field is the average description of the interactions among various atoms in a group of molecules, which has a set of functions and parameters in molecular mechanics and molecular dynamics [18].

All simulations here were based on the Condensed-phase Optimized Molecular Potentials for Atomistic Simulation Studies (COMPASS) force-field [19]. COMPASS, as a member of the consistent force fields (CFF) family, has been widely used in simulation of polymers and supports atomistic simulation of condensed phase materials [20-23]. The force-field parameterization in COMPASS is a combination of *ab initio* parameterization and empirical optimization.

The COMPASS potential function contains bonded, non-bonded, and cross-coupling interaction terms. Bonded interactions include bond stretching, angle bending, dihedral angle torsion, and inversion (improper or out-of-plane) interaction terms. Non-bonded interactions comprise long-range electrostatic and relatively short-range van der Waals (vdW) interactions, as well as hydrogen bonding (H-bonding), implicitly incorporated in other non-bonded terms. Cross-coupling terms present the coupling between different bonded interactions. A typical energy function in CFF is expressed in the following form [19]:

$$
\begin{aligned}
E_{total} = & \sum_{b}[K_2(b-b_0)^2 + K_3(b-b_0)^3 + K_4(b-b_0)^4] \\
& + \sum_{\theta}[H_2(\theta-\theta_0)^2 + H_3(\theta-\theta_0)^3 + H_4(\theta-\theta_0)^4] \\
& + \sum_{\varphi}[V_1[1-\cos(\varphi-\varphi_1^0)] + V_2[1-\cos(2\varphi-\varphi_2^0)] + V_3[1-\cos(3\varphi-\varphi_3^0)]] \\
& + \sum_{X} K_X X^2 + \sum_{b}\sum_{b'} F_{bb'}(b-b_0)(b'-b_0') + \sum_{\theta}\sum_{\theta'} F_{\theta\theta'}(\theta-\theta_0)(\theta'-\theta_0') \\
& + \sum_{b}\sum_{\theta} F_{b\theta}(b-b_0)(\theta-\theta_0) + \sum_{b}\sum_{\varphi}(b-b_0)[V_1\cos\varphi + V_2\cos 2\varphi + V_3\cos 3\varphi] \\
& + \sum_{b'}\sum_{\varphi}(b'-b_0')[V_1\cos\varphi + V_2\cos 2\varphi + V_3\cos 3\varphi] \\
& + \sum_{\theta}\sum_{\varphi}(\theta-\theta_0)[V_1\cos\varphi + V_2\cos 2\varphi + V_3\cos 3\varphi] \\
& + \sum_{\varphi}\sum_{\theta}\sum_{\theta'} K_{\varphi\theta\theta'}\cos\varphi(\theta-\theta_0)(\theta'-\theta_0') + \sum_{i>j}\frac{q_i q_j}{\varepsilon r_{ij}} + \sum_{i>j}[\frac{A_{ij}}{r_{ij}^9} - \frac{B_{ij}}{r_{ij}^6}]
\end{aligned}
\tag{1}
$$

in which, b, θ, and φ are the bond length, bond angle, and dihedral angle, respectively, and b_0, θ_0 , and φ_0 are their equilibrium values during the simulation. The coefficients A, B, C, D, K, H, and V denote the force constants corresponding to various parts of the potential function. The distance between the i^{th} and j^{th} atoms is represented by r_{ij}, and q_i, while q_j shows the electric charges. The parameter ε is the dielectric constant.

Valence terms are described by the first four terms, while cross-coupling terms are represented by the next seven terms. The last two terms are Coulombic and Lennard-Jones (LJ) 9-6 functions, describing the non-bonded interactions including vdW and electrostatic interactions, respectively.

The COMPASS force field was implemented using the Materials Studio software package [24], which was used for all molecular modeling and simulation tasks in this study.

2.2. Preparing the PC/CNT Nanocomposites

In this study, armchair single-walled CNTs (5, 5), respectively, with the diameters of 6.78 Å and 13.56 Å were used as reinforcement. Simulations were performed with different weight fractions of nanotubes. The models used in this study consisted of 1.7 wt%, 2.4 wt%, 4.9 wt%, and 6.9 wt% of (5, 5) nanotubes.

PC was chosen because of its good combination of stiffness and ductility, and its ability to disperse CNTs via melt compounding. PC was made up of bisphenol-A of the formula C16H14O3, as represented in Figure 1.

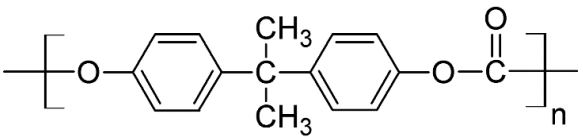

Figure 1. General structure of a polycarbonate (PC) molecule.

Previous studies proved that polymers built with 10 to 15 repeating units can meet the accuracy requirements [25]. Full atomistic models of PC chains, composed of 10 monomers, were created using the polymer builder tool within Materials Studio. CNTs and PC chains were used as input for the construction of PC/CNT nanocomposites.

The nanocomposite RVEs were constructed through randomly-packing the appropriate numbers of polymer chains and carbon nanotubes into the simulation box, so that the target weight fractions of CNTs were achieved. The construction task was performed at room temperature with an initial density of 0.5 g/cm^3 to prevent the build-up of excessive energy within the system during the cell construction, due to ring spearing and catenation of the polymer molecules. The systems were later condensed into the real density at the equilibration step. An instant constructed nanocomposite RVE is depicted in Figure 2.

The periodic boundary conditions were applied to achieve the effect of a bulk environment within the unit cell. An atom-based method, with the cut-off radii of 12.5 Å and a long-range correction, was used in calculation of the vdW interactions. The electrostatic interactions were calculated through the Ewald summation method [26], with an accuracy of 10^{-4} kcal/mol. The number of atoms prepared within the models was in the range of 16600-17380.

2.3. Minimization, Equilibration, and Sampling

The energy of the created structures must be minimized before any subsequent stage of the simulation. The minimization process follows an iterative procedure based on molecular mechanics, in which the coordinates of the atoms and cell parameters are typically adjusted, so the energy of the structure is brought to a local minimum. This phase removes any strong vdW interactions between the atoms, which might otherwise lead to local structural distortion and unstable simulations.

Here, the conjugate gradient method, with a maximum number of iterations limited to 10000 and an energy convergence criterion of 0.001 kcal/mol, was utilized to minimize the energy of the structures. The variations of total energy and convergence versus iteration are plotted in Figure 3, and the comparison of various energy terms before and after minimization appears in Table 1.

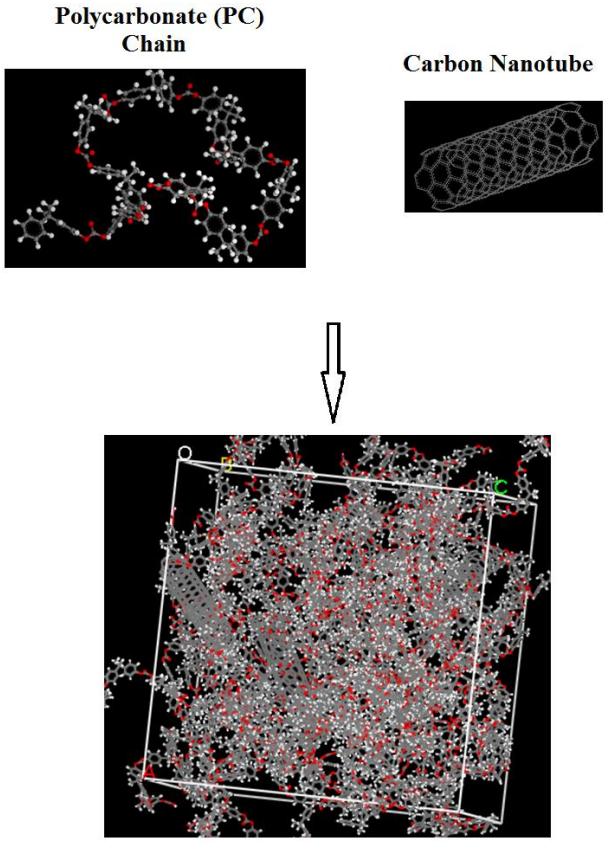

Figure 2. Typical structure of a CNT/PC RVE (6.9 wt%).

Table 1. The energy portions for different contributors to the total energy of the system, before and after minimization

Energy Terms	Energy (kcal/mol)	
	Before Minimization	After Minimization
Total	9932382888.51	-1863.71
Bonded	7979.83	5631.45
Non-Bonded	9932375298.79	-5129.31
Cross-Coupling	-393.85	-2369.60

As shown in Table 1, the non-bonded energy portion was the main contributor to the total energy of the system before minimization, because the atoms are randomly packed into the cells, and therefore can be placed at very short distances from the others. After energy minimization, 500 ps isothermal-isobaric (NPT) dynamics with time step of 1 fs at 298 K and 1 atm was performed, to reach the real density and achieve equilibrium within the system. The Berendsen thermostat and barostat [27] were used to control the temperature and pressure of the system, respectively.

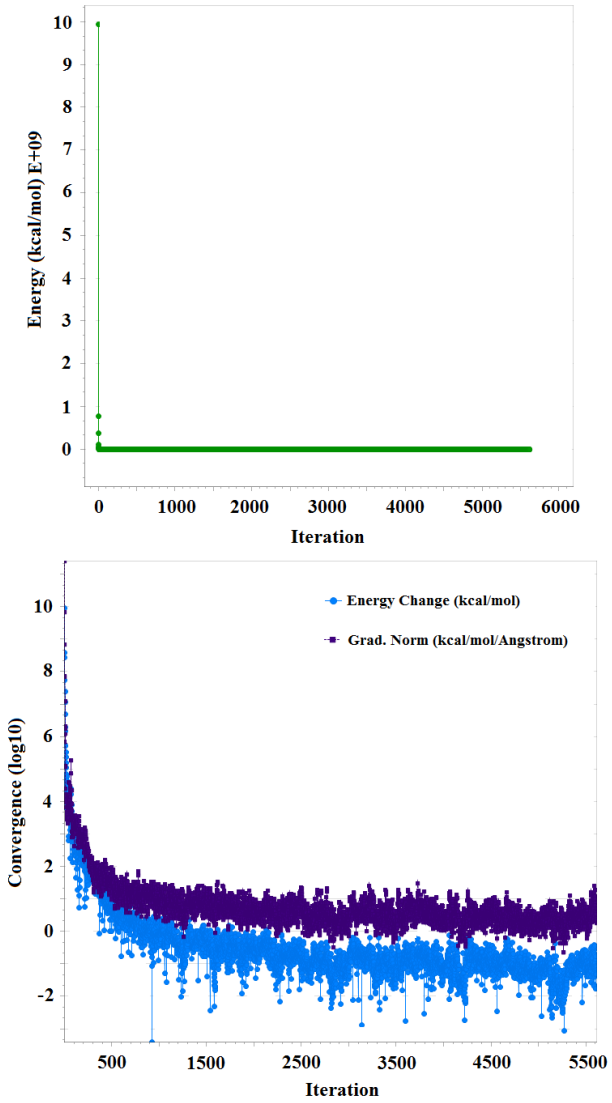

Figure 3. The variations of potential energy and convergence versus iteration in the minimization process.

The time evolutions of the potential energy, temperature, and density of the system were monitored during the dynamics, and the equilibrium state was confirmed as the density reached a constant value with slight fluctuations. For instance, the density of the 6.9 wt% model was converged to 1.17 g/cm^3 after equilibration, as shown in Figure 4. The system was then subjected to 100 ps dynamics through a canonical (NVT) assembly at room temperature to generate sampling trajectories, for prediction material properties in the next step. The Nose-Hoover method [28,29] was applied for controlling the temperature during sampling stage. In each case, configurations were saved as trajectories every 1000 time steps.

2.4. Calculation of Mechanical Properties

Generally speaking, two primary methods are typically used when calculating elastic constants using molecular simulations: the static method, based on molecular mechanics; and the dynamic method. In the current study, the static method was applied, due to its accuracy and reliability. After an initial energy minimization, three pairs of uniaxial tension/compression and three pairs of pure shear deformations within the elastic limits were applied. Each deformation corresponded to a strain pattern (ε), in which one of the components of the strain vector takes a small value of 0.001-0.003 while keeping the other components at zero [30], followed by energy minimization. Each strain pattern, represented in Voigt notation, was converted into the strain matrix (ε), which was then used to generate the metric tensor, G, as follows:

$$G = H_0^T \left[2\varepsilon + I \right] H_0 \tag{2}$$

Here, H_0 is a matrix composed of lattice parameters, while I represents the identity matrix, and H_0^T denotes the transposition of H_0. From G, new lattice parameters were derived, while fractional coordinates were held fixed. Following these steps, the structure was optimized, and the stress was calculated [31,32]. For small deformations, the relationship between stress and strain is represented by

$$\sigma_i = C_{ij} \varepsilon_j \tag{3}$$

where σ_i denotes the components of the stress tensor; C_{ij} are the elastic stiffness coefficients, and ε_j denotes the components of the strain tensor. Therefore, the stiffness matrix was built up from a linear fit between the applied strain and the resulting stress patterns.

Because of the random orientation of CNTs, the material was almost isotropic, for which the elastic stiffness matrix follows a particular pattern, as shown in Eq. (4):

$$C_{ij} = \begin{pmatrix} \lambda+2\mu & \lambda & \lambda & 0 & 0 & 0 \\ \lambda & \lambda+2\mu & \lambda & 0 & 0 & 0 \\ \lambda & \lambda & \lambda+2\mu & 0 & 0 & 0 \\ 0 & 0 & 0 & \mu & 0 & 0 \\ 0 & 0 & 0 & 0 & \mu & 0 \\ 0 & 0 & 0 & 0 & 0 & \mu \end{pmatrix} \tag{4}$$

Thus, the stress-strain relations can be completely described by two Lame constants, λ and μ, calculated from the stiffness constants

$$\lambda = \frac{1}{3}(C_{11}+C_{22}+C_{33}) + \frac{2}{3}(C_{44}+C_{55}+C_{66})$$
$$\mu = \frac{1}{3}(C_{44}+C_{55}+C_{66}) \tag{5}$$

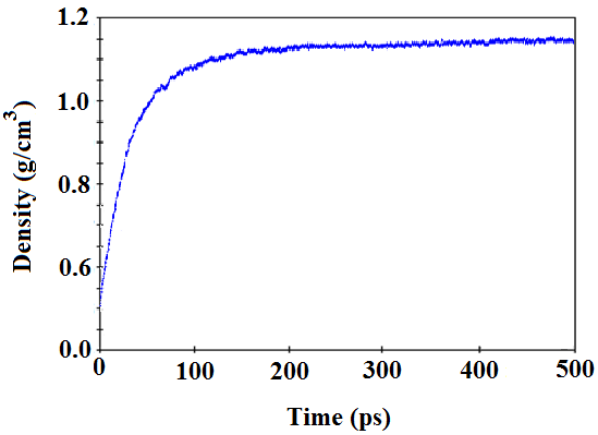

Figure 4. Convergence of density during the simulation for the 6.9 wt% model, as evidence of equilibration.

Finally, the engineering elastic constants can be described in terms of the Lame constants, according to the following equations:

$$E = \mu\frac{3\lambda+2\mu}{\lambda+\mu}$$
$$G = \mu \qquad (6)$$
$$K = \lambda+\frac{2}{3}\mu$$
$$\upsilon = \frac{\lambda}{2(\lambda+\mu)}$$

where *E*, *G*, *K*, and *v* represent the Young's modulus, the shear modulus, the bulk modulus, and Poisson's ratio, respectively.

Applying the above-mentioned procedure, the mechanical properties of pure PC and PC/CNT samples were calculated and averaged over all valid configurations.

3. Results and Discussion

In this section, the results obtained for the atomistic simulation of PC/SWCNT nanocomposite models are presented. The bulk elastic properties of a PC polymer were predicted based on MD simulations. Experimental results for mechanical properties of the pure PC, showed values of 2.35 GPa [5,33], 0.8 GPa [34] and 0.39 [33] for Young's modulus, shear modulus, and Poisson's ratio, respectively, which were in good agreement with the simulation results.

A sample elastic stiffness matrix for one of the nanocomposites reinforced with 2.4 wt% of (5, 5) CNT (length of 32 Å) appears as

$$C_{ij} = \begin{pmatrix} \mathbf{4.82} & \mathbf{2.07} & \mathbf{2.14} & -0.09 & 0.17 & -0.12 \\ \mathbf{2.07} & \mathbf{5.94} & \mathbf{2.89} & -0.08 & -0.09 & 0.10 \\ \mathbf{2.14} & \mathbf{2.89} & \mathbf{3.52} & 0.09 & 0.02 & -0.13 \\ -0.09 & -0.08 & 0.09 & \mathbf{2.48} & 0.19 & -0.08 \\ 0.33 & -0.09 & 0.02 & 0.19 & \mathbf{1.04} & 0.09 \\ -0.12 & 0.09 & -0.13 & -0.08 & 0.09 & \mathbf{0.63} \end{pmatrix}$$

We can confirm that although the non-bolded components of the tensors are not strictly zero, they are dominated by the bolded components, and the deviations of the estimated elastic constants from the values, suggested by Eq. (4), are negligible. Furthermore, all of the stiffness tensors were symmetrical along the diagonal components. Therefore, the calculated elastic stiffness constants reasonably implied the behavior of an isotropic amorphous material.

For nanocomposite models, described in the previous sections, the calculated mechanical properties are reported in Table 2.

The effect of the volume fraction of CNT reinforcements on the mechanical properties of CNT/PC composites is also presented in Table 2. The values for series 1 and series 2 show that when PC is filled with about 4.9 wt% and 6.9 wt% CNTs, Young's modulus improved by 19.4% and 51.7%, respectively, while the shear modulus improved by 26.1% and 60.2%, respectively, when compared to the values for pure PC.

Table 2. Predicted mechanical properties of the polycarbonate reinforced with (5, 5) CNTs.

Models	Series 1 CNT (5, 5) L = 22 Å		Series 2 CNT (5, 5) L = 32 Å		Pure PC
wt%	1.7	4.9	2.4	6.9	0
Cell dimensions (a = b = c)	57.2 Å	40.1 Å	57.3 Å	40.4 Å	57.6 Å
E (GPa)	2.84	3.06	3.62	3.89	2.56
G (GPa)	1.11	1.15	1.33	1.46	0.91
ν	0.28	0.33	0.36	0.33	0.41
K (GPa)	2.15	3.02	4.26	3.85	4.57

Table 3. Type and wt% of the CNTs used in previous studies, presented in Figure 5.

Type of CNT	CNT wt%	Ref.
MWCNT (AR)	2–5	[4]
MWCNT (EP)	2–5	[4]
MWCNT	1–8	[5]
MWCNT	1–5	[35]
SWCNT	1–5	[35]
SWCNT	1–5	[35]
MWCNT	2–8	[36]
MWCNT	0.5–10	[37]
MWCNT (room temp.)	1.5–5	[33]
MWCNT (77 K)	1.5–5	[33]
MWCNT (77 K)	0.1–10	[38]
MWCNT (room temp.)	0.1–10	[38]
MWCNT	0.1–1	[39]
MWCNT (C30)	0.1–1	[39]
MWCNT (C50)	0.1–1	[39]

For validation of the results, the calculated properties were compared with some findings and important results from previous studies on PC/CNT nanocomposites, as depicted in Figure 5. The types and weight fractions of CNTs corresponding to each series of results in Figure 5 are also summarized in Table 3. Current simulation results for series 1 and 2 shown in Figure 5 are presented in yellow and red, respectively, to distinguish them from other results marked with black arrows.

Variation of Young's modulus, with increased CNTs' wt% are plotted in Figure 6, showing a data comparison to a number of studies with the same parameters as the current study.

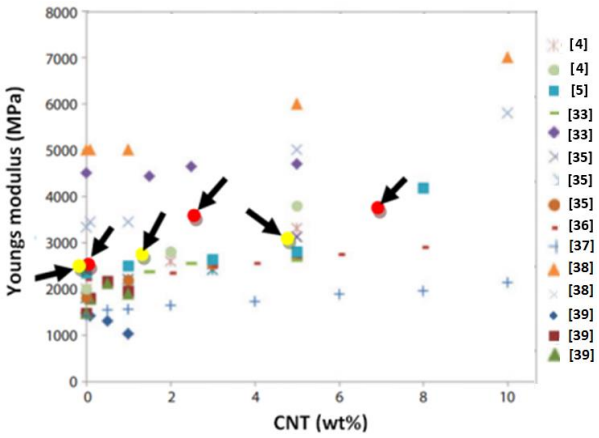

Figure 5. Young's modulus of PC/CNT nanocomposites as a function of CNT content.

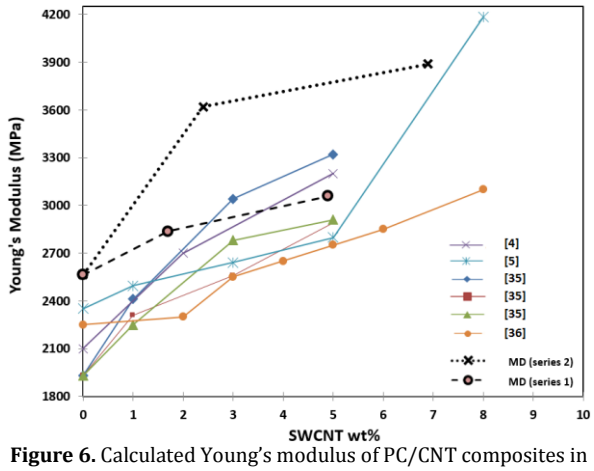

Figure 6. Calculated Young's modulus of PC/CNT composites in comparison to some other experimental results.

Table 4. Variations of Young' moduli of nanocomposites with increasing amounts of CNTs

Models	Increase in SWCNT wt%	Increase in Young's modulus (%)
Series 1	0–1.7	10.7%
	1.7–4.9	7.8%
Series 2	0–2.4	41.2%
	2.4–6.9	7.5%

As shown in the figures, the elastic modulus increased with increased CNT content in the PC matrix, and the predicted modulus was in good agreement with the experimental results. In addition, greater values of Young's modulus were predicted for the series 2 with longer CNTs. The quantitative effects of CNT content on the Young's modulus of nanocomposites is reported in Table 4.

A 52% increase in Young's modulus was seen due to incorporation of 6.9 wt% SWCNT when compared to pure PC. However, beyond a certain amount of CNT content, the reinforcement effect was reduced. This behavior is attributed to the proper dispersion of CNTs at lower weight ratios, which consequently led to stronger π-π interaction between CNTs and the matrix, the combination of large aspect ratios and high surface-to-volume ratios of CNTs, and improved load transfer capability of SWCNTs. However, for higher weight ratios, aggregation of CNTs prevented significant improvement of the mechanical properties [3].

The relatively high predicted mechanical properties from the simulations followed a trend similar to that observed in the literature. In the current study, the predicted properties were slightly higher than those reported in experimental studies, which was due to the fact that in molecular simulations, properties are calculated for a nearly perfect uniform molecular structure, whereas, under real experimental conditions, the materials may contain air pockets, impurities, and unreacted monomers. Additionally, previous studies have shown that nanotube imperfections or defects significantly reduced the mechanical properties of CNT-reinforced nanocomposites [40,41].

Variations of the shear modulus with respect to SWCNT weight percentages demonstrated the increase in the shear modulus, when the SWCNT volume fraction increased from 0% to 1.7%, and from 1.7% to 2.4%, respectively, for the series 1 and series 2 models. This increase was steeper than the increase when the CNT volume fraction increased from 1.7% to 4.9% for series 1, and from 2.4% to 6.9% for series 2. The aspect ratio (l/d) of CNTs played an important role in the final mechanical properties of polymer/CNT composites. In this study, the effect of the aspect ratio of carbon nanotubes on the mechanical behavior of PC/CNT was investigated for two aspect ratios—1.6 and 6.2, and a weight fraction of 3.2%. This study found that the elastic moduli increased with increasing the CNT aspect ratio.

4. Conclusions

In this study, PC/SWCNT nanocomposites were modeled at the atomic scale, and the engineering properties of the material were estimated through the MD method. This research investigated the influence of geometry, aspect ratio, and weight fraction of CNTs on the elastic properties of nanocomposites. The results indicated that mechanical properties of PC were greatly enhanced by incorporating carbon nanotubes. A significant increase in the elastic modulus (up to 52%) was observed with the addition of only 6.9 wt% of SWCNTs. Also, upon addition of about 2.4 wt% of SWCNTs, the elastic modulus increased by almost 41.2%. In most cases, when the CNT weight fraction increased up to 3%, the improvement in elastic modulus was greater than that for wt% higher than 3%. Higher CNT aspect ratios (l/d) led to enhanced mechanical properties of nanocomposites. The predicted results were in good agreement with the experimental observations.

Acknowledgements

The High Performance Computing Center of Amirkabir University of Technology (HPCRC), Tehran, Iran is acknowledged for providing computational facilities for our simulations.

References

[1] Dar UA, Zhang W, Xu Y, Wang J. Thermal and strain rate sensitive compressive behavior of polycarbonate polymer-experimental and constitutive analysis. *J Polymer Research* 2014; 21(8): 1-10

[2] Mittal V. **Polymer Nanotubes Nanocomposites: Synthesis, Properties and Applications**. John Wiley and Sons, 2014

[3] Sharma S, Chandra R, Kumar P, Kumar N. Thermo-mechanical characterization of multi-walled carbon nanotube reinforced polycarbonate composites: A molecular dynamics approach. *Comptes Rendus Mécanique* 2015; 343(5): 371-396

[4] Eitan A, Fisher F, Andrews R, Brinson L, Schadler L. Reinforcement mechanisms in MWCNT-filled polycarbonate. *Compos Sci Technol* 2006; 66(9): 1162-1173

[5] Chen L, Pang X-J, Yu Z-L. Study on polycarbonate/multi-walled carbon nanotubes composite produced by melt processing. *Mater Sci Eng, A* 2007; 457(1): 287-291

[6] Aghadavoudi F, Golestanian H, Tadi Beni Y. Investigating the Effects of Resin Cross-Linking Ratio on Mechanical Properties of Epoxy-Based Nanocomposites Using Molecular Dynamics. *Polym Compos* 2016; doi:10.1002/pc.24014

[7] Arash B, Wang Q, Varadan VK. Mechanical properties of carbon nanotube/polymer composites. *Sci Rep* 2014; 4: 1-8

[8] Sharma S, Chandra R, Kumar P, Kumar N. Thermo-mechanical characterization of multi-walled carbon nanotube reinforced polycarbonate composites: A molecular dynamics approach. *Comptes Rendus Mecanique* 2015; 343(5-6): 371-396

[9] Gates T, Odegard G, Frankland S, Clancy T. Computational materials: multi-scale modeling and simulation of nanostructured materials. *Compos Sci Technol* 2005; 65(15): 2416-2434

[10] Odegard G, Gates T, Wise K, Park C, Siochi E. Constitutive modeling of nanotube-reinforced polymer composites. *Compos Sci Technol* 2003; 63(11): 1671-1687

[11] Odegard GM, Gates TS, Nicholson LM, Wise KE. Equivalent-continuum modeling of nano-structured materials. *Compos Sci Technol* 2002; 62(14): 1869-1880

[12] Rossi M, Meo M. On the estimation of mechanical properties of single-walled carbon nanotubes by using a molecular-mechanics based FE approach. *Compos Sci Technol* 2009; 69(9): 1394-1398

[13] Papanikos P, Nikolopoulos D, Tserpes K. Equivalent beams for carbon nanotubes. *Comput Mater Sci* 2008; 43(2): 345-352

[14] Tserpes K, Papanikos P, Labeas G, Pantelakis SG. Multi-scale modeling of tensile behavior of carbon nanotube-reinforced composites. *Theoretical and Applied Fracture Mechanics* 2008; 49(1): 51-60

[15] Valavala PK, Odegard GM, editors. Multiscale constitutive modeling of polymer materials. ASME International Mechanical Engineering Congress and Exposition; 2007: American Society of Mechanical Engineers

[16] Guglielmi M, Kickelbick G, Martucci A. **Sol-Gel Nanocomposites**. Springer, 2014

[17] Frenkel D, Smit B. Understanding molecular simulations: from algorithms to applications. Academic Press, 1996

[18] Al-Ostaz A, Pal G, Mantena PR, Cheng A. Molecular dynamics simulation of SWCNT–polymer nanocomposite and its constituents. *J Mater Sci* 2008; 43(1): 164-173

[19] Sun H. COMPASS: an ab initio force-field optimized for condensed-phase applications overview with details on alkane and benzene compounds. *J Phys Chem B* 1998; 102(38): 7338-7364

[20] Fried J. The COMPASS force field: parameterization and validation for phosphazenes. *Comput Theor Polym Sci* 1998; 8(1-2): 229-246

[21] Bunte SW, Sun H. Molecular modeling of energetic materials: the parameterization and validation of nitrate esters in the COMPASS force field. *J Phys Chem B* 2000; 104(11): 2477-2489
[22] Yang J, Ren Y, Tian A-m, Sun H. COMPASS force field for 14 inorganic molecules, He, Ne, Ar, Kr, Xe, H2, O2, N2, NO, CO, CO2, NO2, CS2, and SO2, in liquid phases. *J Phys Chem B* 2000; 104(20): 4951-4957
[23] McQuaid MJ, Sun H, Rigby D. Development and validation of COMPASS force field parameters for molecules with aliphatic azide chains. *J Comput Chem* 2004; 25(1): 61-71
[24] http://accelrys.com/products/collaborative-science/biovia-materials-studio/
[25] Yang S, Choi J, Cho M. Elastic stiffness and filler size effect of covalently grafted nanosilica polyimide composites: Molecular dynamics study. *ACS Appl Mater Interfaces* 2012; 4(9): 4792-4799
[26] Ewald PP. Die Berechnung optischer und elektrostatischer Gitterpotentiale. *Ann Phys* 1921; 369(3): 253-287
[27] Berendsen HJ, Postma Jv, van Gunsteren WF, DiNola A, Haak J. Molecular dynamics with coupling to an external bath. *J Chem Phys* 1984; 81(8): 3684-3690
[28] Nosé S. A molecular dynamics method for simulations in the canonical ensemble. *Mol Phys* 1984; 52(2): 255-268
[29] Hoover WG. Canonical dynamics: equilibrium phase-space distributions. *Physical Review A* 1985; 31(3): 1695
[30] Materials Studio 6.0 (Accelrys Inc.), Classical simulations theory – mechanical properties
[31] Shokuhfar A, Arab B. The effect of cross linking density on the mechanical properties and structure of the epoxy polymers: molecular dynamics simulation. *J Molecul Modell* 2013; 19(9): 3719-3731
[32] Arab B, Shokuhfar A. Molecular dynamics simulation of cross-linked urea-formaldehyde polymers for self-healing nanocomposites: prediction of mechanical properties and glass transition temperature. *J Molecul Modell* 2013; 19(11): 5053-5062
[33] Takeda T, Shindo Y, Narita F, Mito Y. Tensile characterization of carbon nanotube-reinforced polymer composites at cryogenic temperatures: experimens and multiscale simulations. *Mater Trans* 2009; 50(3): 436-445
[34] Christopher WF, Fox DW. **Polycarbonates**. Reinhold Publishing Corporation, 1962
[35] Fornes T, Baur J, Sabba Y, Thomas E. Morphology and properties of melt-spun polycarbonate fibers containing single-and multi-wall carbon nanotubes. *Polym* 2006; 47(5): 1704-1714
[36] King JA, Via MD, Caspary JA, Jubinski MM, Miskioglu I, Mills OP, et al. Electrical and thermal conductivity and tensile and flexural properties of carbon nanotube/polycarbonate resins. *J Appl Polym Sci* 2010; 118(5): 2512-2520
[37] Man Y, Li Z, Zhang Z. Interface-dependent mechanical properties in MWNT-filled polycarbonate. *Mater Trans* 2009; 50(6): 1355-1359
[38] Oliver A, Bult J, Le QV, Mbaruku AL, Schwartz J. Mechanical properties of non-functionalized multiwall nanotube reinforced polycarbonate at 77 K. *Nanotechnol* 2008; 19(50): 505702
[39] Kim KH, Jo WH. A strategy for enhancement of mechanical and electrical properties of polycarbonate/multi-walled carbon nanotube composites. *Carbon* 2009; 47(4): 1126-1134
[40] Islam MZ, Mahboob M, Lowe RL. Mechanical properties of defective carbon nanotube/polyethylene nanocomposites: A molecular dynamics simulation study. *Polym Compos* 2014; 37(1): 305-314
[41] Aghadavoudi F, Golestanian H, Beni YT. Investigation of CNT Defects on Mechanical Behavior of Cross linked Epoxy based Nanocomposites by Molecular Dynamics. *Int J Adv Design Manuf Technol* 2016; 9(1): 137-146